JOURNAL OF MATERIALS SCIENCE 32 (1997) 1591–1597

An extended X-ray absorption fine structure investigation on the local environment of niobium ions in Nb_2O_5-doped $SrTiO_3$ glass ceramics

G. MOSEL, M. WILLFAHRT, U. BANACH, Th. HÜBERT
Federal Institute for Materials Research and Testing (BAM), Unter den Eichen 44–46, D-12203 Berlin, Germany

The dielectrical properties of glass ceramics derived from $SrO–B_2O_3–Al_2O_3–TiO_2$ glasses are improved by doping the starting material with Nb_2O_5 and judicious choice of heat treatment conditions. In order to understand this effect the local environment of the niobium ions is studied by EXAFS (extended X-ray absorption fine structure) investigations at the Nb-*K* edge. For comparison purposes Ti-*K* and Sr-*K* EXAFS spectra have also been measured. The experiments suggest that the niobium ions are incorporated onto titanium sites in the crystalline $SrTiO_3$ phase formed during the thermal treatment.

1. Introduction

The dielectrical constant ε_{rel} of glass ceramics based on the system $SrO–B_2O_3–Al_2O_3–TiO_2$ are substantially improved by doping the initial material with up to 5 mol % Nb_2O_5. Judicious choice of the heat treatments can result in glass ceramics with high dielectric constants $\varepsilon_{rel} \geqslant 5000$, which show a monotonic behaviour of $\varepsilon_{rel}(T)$ down to about 4 K. Thus, these ceramics are promising candidates for application as capacitive temperature sensors in the range of 4–100 K [1, 2]. During the thermal treatment of the glass obtained from the melt the crystalline phases $Sr_2Ti_5O_{12}$ (metastable), $SrTiO_3$ (cubic perovskite structure) and TiO_2 (rutile) are formed in the glass ceramics [3]. X-ray diffraction experiments have shown that Nb_2O_5-doping caused an expansion of the $SrTiO_3$ lattice (a_0 increased from 0.3905 nm in the undoped to 0.3928 nm in the material doped with 5 mol % Nb_2O_5) [4]. We assume the formation of a solid solution where the Nb ions occupy titanium sites to explain the observed lattice expansion since the Nb ions are larger than the Ti ions they are replacing.

Because of the low Nb concentration involved in the doping information about the Nb local environment cannot be derived from the total radial distribution functions obtained by wide angle X-ray scattering (WAXS). To verify the hypothesis previously presented (Nb ions on Ti sites) a partial radial distribution function (PRDF) describing the Nb environment has to be determined. This PRDF may be easily derived from the Nb-*K* extended X-ray absorption fine structure (EXAFS) spectrum.

We report an EXAFS investigation at the Nb-*K* and the Ti-*K* absorption edges which presents evidence for the incorporation of Nb ions on Ti sites in the $SrTiO_3$ phase formed during the thermal treatment.

2. Experimental procedure

2.1. Sample preparation

The glasses were obtained from a melt with the composition of 34 SrO-25 B_2O_3-7 Al_2O_3-34 TiO_2 (in mol %) to which 0.5, 2.5, and 5.0 mol % Nb_2O_5, respectively, were added.

The glasses for the EXAFS investigations were submitted to a "slow" ($10\ K\ min^{-1}$) and a "fast" ($100\ K\ min^{-1}$) heating up to 850 °C, held at this temperature for 15 min and cooled down to 50 °C in the furnace. The precipitated solid solution phase was extracted from the glassy matrix by lixiviation in nitric acid. Pure samples of $SrTiO_3$ and Nb_2O_5 were used as crystalline reference compounds.

The room temperature EXAFS measurements were performed at the Ti-*K*, Sr-*K*, and Nb-*K* edges in transmission mode at HASYLAB at DESY (Hamburg) on beamlines EXAFS II and RÖMO II. Details are given in Table I.

2.2. EXAFS spectroscopy

During their passage through matter X-ray photons interact with any encountered atoms. If the photon energy *E* exceeds the binding energy of the electrons in a core shell of an encountered atom then this shell may become ionized which leads to the absorption of the photon and the emission of a photoelectron. The outgoing photoelectron wave is backscattered by the atoms in the neighbourhood of the absorbing atom. The outgoing and backscattered waves interfere and

0022–2461

TABLE I Samples, preparation and measured EXAFS spectra

Sample compositions and preparation	Measured spectra	Label in Figs 1–3
Nb_2O_5, powdered, crystalline	Nb-*K*	1N
Glass containing 2.5 mol % Nb_2O_5, not tempered	Nb-*K*, Sr-*K*	2N, 2S
Glass ceramic containing 2.5 mol % Nb_2O_5, fast tempered	Nb-*K*, Sr-*K*	3N, 3S
Glass ceramic containing 2.5 mol % Nb_2O_5, fast tempered and lixiviated	Nb-*K*, Ti-*K*, and Sr-*K*	4N, 4T, 4S
Glass ceramic containing 2.5 mol % Nb_2O_5, slow tempered	Nb-*K*, Sr-*K*	5N, 5S
$SrTiO_3$, powdered, crystalline	Ti-*K*, Sr-*K*	6T, 6S
Glass containing 5.0 mol % Nb_2O_5, not tempered	Nb-*K*, Sr-*K*	7N, 7S
Glass ceramic containing 5.0 mol % Nb_2O_5, fast tempered	Nb-*K*, Sr-*K*	8N, 8S
Glass ceramic containing 0.5 mol % Nb_2O_5, fast tempered	Nb-*K*, Sr-*K*	9N, 9S

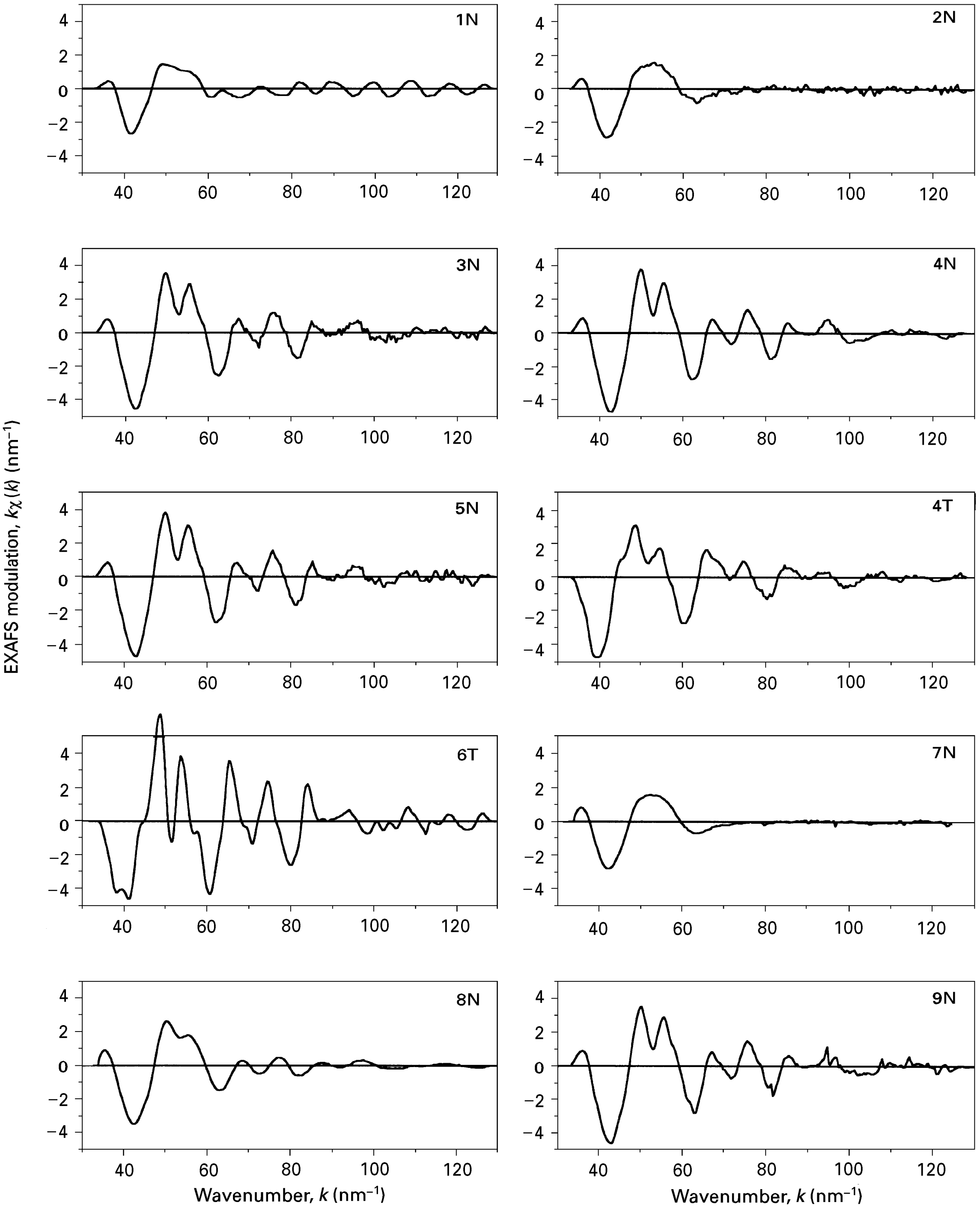

Figure 1 Nb-*K* and Ti-*K* EXAFS modulations $k \cdot \chi(k)$ (sample labelling as in Table I).

this leads to slight modulations of the absorption coefficient $\mu(E)$ which may be extracted from the spectra using standard procedures (Victoreen fit, spline interpolation). The resulting EXAFS modulations $\chi(k)$ (Fig. 1) where k is the wavenumber, contain information on the local environment of the absorbing atom (interatomic distances R_j, coordination numbers N_j and Debye–Waller factors $\exp(-2\sigma_j^2 k^2)$ with σ_j^2 being the mean square deviation of R_j). Fourier transforming the EXAFS modulation results in a pseudo-PRDF $|F(r)|$ which gives a one-dimensional image of the environment of the absorbing atom. The peaks appearing in the $|F(r)|$ can be related to the coordination shells of the absorbing atom. However, the positions of the peak maxima do not coincide with the real interatomic distances. Because of a phase shift of the photoelectron wave during its trip from the absorbing atom to the neighbouring atoms and back, the peaks are shifted to lower distances by *circa* 0.03–0.05 nm. To determine exact interatomic distances a parameter fit using structurally known crystalline standards has to be performed.

3. Discussion of the Fourier transforms

3.1. Crystalline reference compounds

The magnitudes of the Fourier transforms $|F(r)|$ of the crystalline reference samples $SrTiO_3$ (Ti-*K* spectrum, label 6T) and Nb_2O_5 (Nb-*K* spectrum, label 1N), which are shown in Fig. 2a, will serve as the starting point of the discussion. $SrTiO_3$ has a highly symmetrical, cubic structure (perovskite) with a lattice constant $a = 0.3905$ nm. In the Fourier transform of its Ti-*K* spectrum the local order of the Ti^{4+} ions is visible up to the seventh coordination shell (Table II).

On the other hand, the Fourier transform of Nb_2O_5 (1 N) is far less structured. Only an asymmetrical peak at 0.35 nm corresponding to the shortest Nb–Nb correlation is visible. The first coordination sphere of the Nb^{5+} ions (6 oxygens at a mean distance of about 0.19 nm) is nearly invisible in the $|F(r)|$ (absence of a peak at about 0.16 nm). This attenuation is due to the low crystalline symmetry of the Nb_2O_5. The distribution of the Nb–O distances in the Nb_2O_5 structure (monoclinic) is very broad (minimum: 0.173 nm, maximum: 0.246 nm). Consequently, the interference of the backscattered electron waves is to a high degree destructive, leading to the absence of the peak expected at 0.16 nm.

3.2. Glasses and glass ceramics containing 2.5 mol % Nb_2O_5

The Nb-*K* $|F(r)|$ of the untempered glass (2N) displays only weak structures in the range of the first coordination shell of niobium, which are similar to those of crystalline Nb_2O_5. Thus, Nb ions should be incorporated into the glass structure in a disordered manner with a broad distribution of the Nb–O distances, similar to Nb_2O_5. A Nb-cation correlation which would produce a peak at 0.35 nm (as in Nb_2O_5) cannot be detected, indicating the absence of crystalline Nb_2O_5 in the glass.

The thermal treatment of the initial glass causes striking changes in the Fourier transforms of the resulting ceramics. The $|F(r)|$ of all the tempered samples (3N, 4N, 5N) unambiguously indicate, that the Nb ions incorporated into the $SrTiO_3$ phase occupy Ti sites. This is concluded from the now distinctly marked peak at 0.156 nm (corresponding to

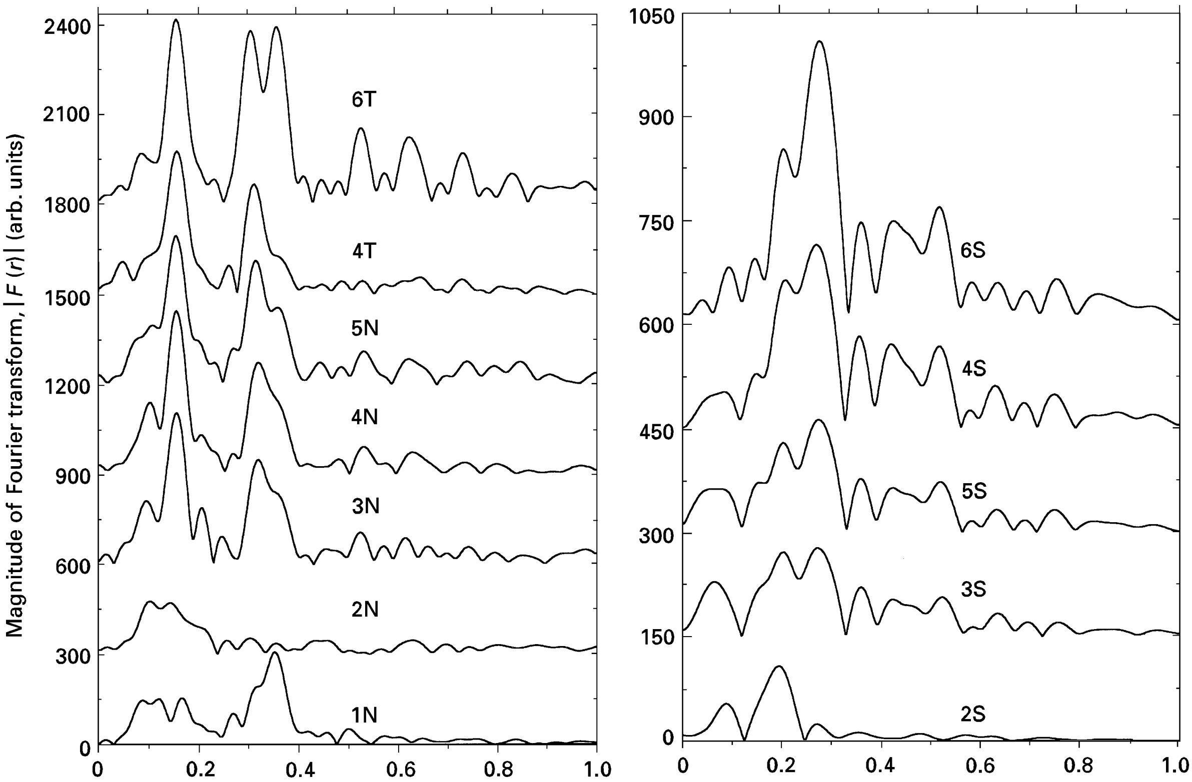

Figure 2 Fourier transforms of the glasses containing 2.5 mol % Nb_2O_5: (a) Nb-*K* and Ti-*K*, (b) Sr-*K*. For comparison, the $|F(r)|$ of crystalline Nb_2O_5 and $SrTiO_3$ are also shown. Transformed *k* ranges: $30 < k < 130\ \text{nm}^{-1}$ for Nb and Ti spectra, $20 < k < 95\ \text{nm}^{-1}$ for Sr spectra. The key to the labels is contained in Table I.

TABLE II Peak positions and related co-ordination spheres (Ti local environment in crystalline $SrTiO_3$). Oxygen atoms beyond the first co-ordination sphere have been neglected because of their very low scattering contributions

Position of the peak maximum (nm)	Real distance between Ti and neighbouring atom (nm)	Coordination number and type of neighbours
0.158	0.1953	6 O
0.306	0.3382	8 Sr
0.358	0.3905	6 Ti
0.526	0.5523	12 Ti
0.623	0.6476 and 0.6764	24 Sr and 8 Ti (superposition)
0.731	0.7810	6 Ti
0.831	0.8732	24 Sr

the first coordination shell of niobium). Its position and shape are very similar to those of the first peak in the Ti-*K* Fourier transform of polycrystalline $SrTiO_3$ (6T). Moreover, the second and third co-ordination shell of Nb in the glass and Ti in $SrTiO_3$ are also similar in that: the double peak structure in the Ti-$K|F(r)|$ of $SrTiO_3$ (maxima at 0.306 and 0.358 nm) also appears in the Nb-$K|F(r)|$ of the glass ceramics. However, both peaks are not clearly separated in this case but in fact strongly superpose. This is due to a slightly distorted crystal structure (as compared to $SrTiO_3$).

Curve 4N displays the $|F(r)|$ of the Nb-*K* spectrum of the purely crystalline phases which were obtained from the fast tempered ceramic via lixiviation. Compared to the $|F(r)|$ of its unlixiviated precursor (3N) the features typical for $SrTiO_3$ appear somewhat more distinctly, since the background from the Nb ions remaining in the glassy matrix is suppressed. The intensity of the double peak structure in the range 0.25–0.40 nm is increased by about 10% and two weak peaks (corresponding to distant Ti-cation co-ordination shells in $SrTiO_3$) appear at 0.53 and 0.63 nm, respectively. This is evidence for the incorporation of Nb ions on to Ti sites in the doped $SrTiO_3$ phase formed. Since the intensities of the main peaks (in the range $r < 0.4$ nm) increase by about 10%, we assume a correspondingly low Nb_2O_5 concentration in the matrix. About 90% of the Nb ions are located in the $SrTiO_3$ phase. Additionally, the Ti-*K* spectrum (4T) was measured for this lixiviated sample thereby allowing a direct comparison of both Ti and Nb local environments. Differences appear in the shapes of the double peak structures in the range from 0.25–0.40 nm (Table III). In the Ti-*K* Fourier transform of the $SrTiO_3$ reference sample both parts of the structure form well-separated peaks at 0.306 and 0.358 nm. In the tempered glasses, however, the two peaks strongly superpose. In the Ti-*K* Fourier transform of the lixiviated sample (4T) the second part of this structure (at about 0.36 nm) is only visible as a low-lying shoulder, whereas it is observed as a much higher shoulder in the Nb-*K* Fourier transform (4N). The reason for the significant intensity difference for the structure at 0.36 nm (corresponding to the third co-ordination shell of Nb and Ti, respectively) is a focusing effect in the case of collinearly arranged atoms, which occurs in the EXAFS spectra of many crystalline compounds. In the ABO_3 perovskite structure the B atoms (here Ti, Nb) are octahedrally surrounded by 6 O atoms in the first shell, hexahedrally by 8 A atoms (here Sr) in the second shell and octahedrally again by 6 B atoms (here Ti, Nb) in the third co-ordination shell. Thus, the central B atom, the O atoms of the first shell and the B atoms of the third shell are in collinear arrangement. The O atoms are acting as lenses amplifying the scattering contributions from the B atoms in the third co-ordination shell and the corresponding structure in the Fourier transform at about 0.36 nm. Slight distortions of the collinear arrangement may cause a significant weakening of the focusing effect which may diminish the related peak. This may explain the significant differences in the intensities of the structure at 0.36 nm in the $|F(r)|$ observed for the investigated samples.

To eliminate phase shift effects, a parameter fit was performed for the first co-ordination shell of all the samples. During the fit the interatomic distance (Ti–O and Nb–O, respectively) and the related Debye–Waller factors were allowed to vary, while the co-ordination number was fixed at six (because of the octahedral environment). The results of this procedure are presented in Table IV. A fit for the second and third co-ordination shells would also be desirable, however is very difficult to perform because of the strong superposition of the two related peaks and also multiple scattering effects that are difficult to handle.

Striking changes of the double peak structure are visible in the Nb-*K* Fourier transform of the slow tempered glass (5N) in that its high-*r* part (due to the third co-ordination shell), which was visible only as a shoulder in the fast tempered glasses, is now well-separated from the peak of the second co-ordination shell. The maxima of both peaks occur at 0.315 and 0.359 nm, whereas they were found at 0.306 and 0.358 nm in the Ti-*K* Fourier transform of $SrTiO_3$. These shifts may indicate a lattice expansion in the Nb-doped $SrTiO_3$ structure, which has also been observed in X-ray diffraction (XRD) experiments [4]. However, these peak positions (given in Table III) are not corrected for scattering phase shifts and therefore cannot be used to quantitatively determine the lattice expansion.

The Ti–O distance in the fast tempered and lixiviated glass (4T) could be accurately detected (± 0.001 nm), since a suitable standard (polycrystalline $SrTiO_3$) was available. Such a standard was unavailable for the Nb–O distances. Therefore we had to use theoretical phase shifts [5], which lead to larger

TABLE III Peak positions for the first, second and third co-ordination shells (CS) in the $|F(r)|$ of the tempered glasses

Sample	Spectrum	Label	Peak position of the 1st CS (nm)	Peak position of the 2nd CS (nm)	Peak position of the 3rd CS (nm)
Fast tempered	Nb-*K*	3N	0.156	0.319	~ 0.36 (shoulder)
Fast tempered, lixiviated	Nb-*K*	4N	0.157	0.319	~ 0.36 (shoulder)
Slow tempered	Nb-*K*	5N	0.156	0.315	0.359
Fast tempered, lixiviated	Ti-*K*	4T	0.158	0.312	~ 0.36 (shoulder)
$SrTiO_3$, polycrystalline	Ti-*K*	6T	0.158	0.306	0.358

TABLE IV Peak positions and interatomic distances (Nb–O and Ti–O, respectively) obtained by parameter fitting for the first coordination shells (CS) in the $|F(r)|$ of the tempered glasses. Polycrystalline $SrTiO_3$ has been used as a standard

Sample	Spectrum	Label	Peak position of the 1st CS (nm)	Real interatomic distance R(nm)	Mean square deviation σ^2 (nm^2)
Fast tempered	Nb-*K*	3N	0.156	0.199 ± 0.003	5.4×10^{-5}
Fast tempered, lixiviated	Nb-*K*	4N	0.157	0.199 ± 0.003	3.4×10^{-5}
Slow tempered	Nb-*K*	5N	0.156	0.199 ± 0.003	4.0×10^{-5}
Fast tempered, lixiviated	Ti-*K*	4T	0.158	0.195 ± 0.001	3.0×10^{-5}
$SrTiO_3$, polycrystalline	Ti-*K*	6T	0.158	0.19525	3.0×10^{-5}

error limits ($\pm$ 0.003 nm) for the calculated distances. The results presented in Table IV indicate that the Nb–O distance in the Nb-containing $SrTiO_3$ phase is about 0.004 nm larger than the Ti–O distance, which remains unchanged compared to pure $SrTiO_3$. In the X-ray diffraction experiments an expansion in the lattice constant of only $\Delta a = +0.0013$ nm was detected. Thus, the EXAFS results reveal, that (because of the larger Nb ionic radius compared to Ti) the lattice is mainly expanded in the Nb environment leading to the slight overall lattice expansion observed by X-ray diffraction. This expansion enables increased shifts of titanium and niobium ions (relative to Sr ions) under the influence of an electric field, i.e., a higher dielectric polarizibility. Indeed, much higher dielectric constants were observed in the Nb-doped ceramics compared to Nb-free samples [4].

Taking into account the Sr-*K* Fourier transforms in Fig. 2b, we are able to estimate the nominal Sr:Nb ratio in the Nb-doped $SrTiO_3$ phase formed. The typical $SrTiO_3$ features are present in all tempered samples containing 2.5 mol % Nb_2O_5, but with very different intensities. Lixiviation of the fast tempered glass, which led to only slightly enhanced peaks (by about 10%) in the Nb-*K* Fourier transform (3N, 4N), causes an increase of the peak intensities in the Sr-*K* Fourier transform (3S, 4S) by a factor of *circa* 2. From this increase we conclude, that during fast tempering only about 50% of the Sr ions are locked into the $SrTiO_3$ phase, with the remainder staying in the glassy matrix. On the other hand, as estimated above, about 90% of the available Nb ions are incorporated into the $SrTiO_3$ phase. From these percentages and the initial glass composition given above (34 mol % SrO, 2.5 mol % Nb_2O_5 and further components) we obtain an atomic Sr:Nb ratio of 3.7 $\pm$ 1.0, which should be present in the Nb-doped $SrTiO_3$ phase.

3.3. Changes of the Nb local order depending on the Nb_2O_5 concentration

Fig. 3 (a and b) shows the Nb-*K* and Sr-*K* Fourier transforms of the fast tempered glasses containing 0.5, 2.5 and 5.0 mol % Nb_2O_5, respectively. Additionally, the Fourier transforms of the untempered glass containing 5.0 mol % Nb_2O_5 and $SrTiO_3$ (Sr-*K*) are presented. From the first peak in the Nb-*K* transforms (maximum at 0.15–0.16 nm) the content of Nb ions inserted into the $SrTiO_3$ phase (on Ti sites) may be estimated. The peak parameters required are given in Table V.

It should be noted that the peak areas are only approximately proportional to the concentration of Nb ions in the $SrTiO_3$ phase, since they are highly sensitive to deviations from the ideal cubic structure of $SrTiO_3$. To treat these deviations exactly, a parameter fitting of the EXAFS modulations $k \cdot \chi(k)$ would be necessary. However the general tendencies may be detected, via the following simple peak analysis, which is valid under the assumption that the local symmetries of the Ti and Nb ions forming the Nb-doped $SrTiO_3$ phase are identical. We further assume, that the peak intensities are solely determined by the oxygen backscattering amplitude, and not by the type of the absorbing atom (Ti or Nb).

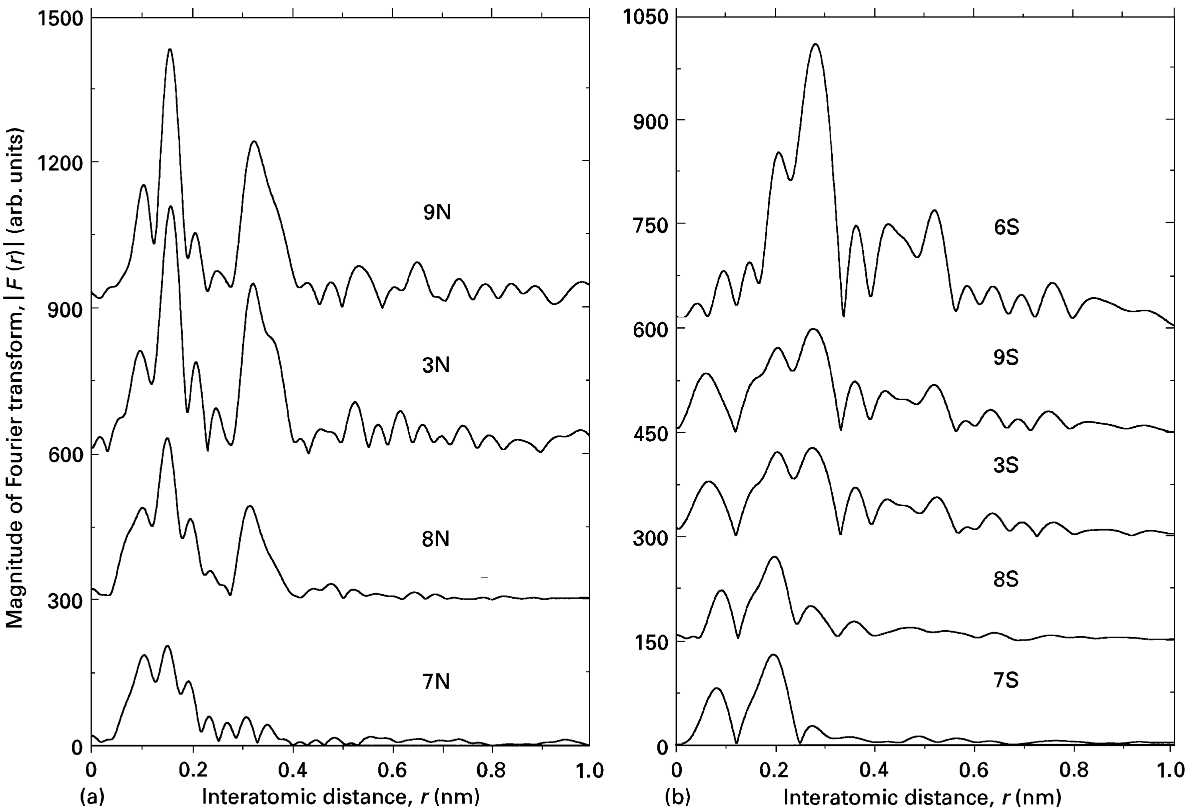

Figure 3 Fourier transforms of the fast tempered glasses containing 0.5, 2.5, and 5.0 mol % Nb_2O_5 and the untempered glass with 5 mol % Nb_2O_5: (a) Nb-*K*, (b) Sr-*K*. The Sr-*K* Fourier transform of $SrTiO_3$ is presented for comparison. The key to the labels is contained in Table I.

TABLE V Parameters of the peaks in the $|F(r)|$ of the glasses containing different amounts of Nb_2O_5. The peak areas (peak height multiplied by the full width at half maximum (FWHM)) are related to the area of the $SrTiO_3$ peak (= 100)

Sample	Peak height (arb. units)	FWHM (nm)	Peak area (rel. units)
$SrTiO_3$, polycrystalline	623	0.048	100
Glass, fast tempered 0.5 mol % Nb_2O_5	534	0.044	79
Glass, fast tempered 2.5 mol % Nb_2O_5	509	0.047	80
Glass, fast tempered 5.0 mol % Nb_2O_5	334	0.047	52

A comparison of the peak areas presented in Table V reveals that in the glasses containing 0.5 and 2.5 mol % Nb_2O_5, (80 ± 10)% of the available Nb ions are incorporated into the $SrTiO_3$ phase formed during the thermal treatment. In the glass containing 5.0 mol % Nb_2O_5 this portion is significantly lower: (52 ± 10)%. The structure in the range 0.25–0.40 nm (corresponding to the second and third co-ordination shells) also decreases. A similar decrease of the amount of crystalline $SrTiO_3$ is visible in the Sr-*K* spectra. While the $SrTiO_3$-like features are well reflected in the $|F(r)|$ of the samples with 0.5 and 2.5 mol % Nb_2O_5, they are drastically diminished in the sample containing 5.0 mol % Nb_2O_5. The percentage of Sr ions in a $SrTiO_3$-like environment should only be (20 ± 5)% in this sample.

These features indicate that Nb_2O_5 concentrations higher than 2.5 mol % hinder the formation of crystalline $SrTiO_3$. We assume a saturation of the $SrTiO_3$ phase by Nb ions beginning at Nb_2O_5 concentrations between 2.5–3.0 mol %. Excess Nb ions can no longer be incorporated on the Ti sites of the $SrTiO_3$ phase. An increase of the Nb_2O_5 concentration causes an enhancement of the content of Nb ions in the glassy matrix, where they occupy strongly distorted octahedral sites (as in crystalline Nb_2O_5 and in numerous niobates). They may tend to form strontium niobate phases, causing a decrease of the Sr ions available for the formation of $SrTiO_3$. This result is in agreement with X-ray diffraction studies, which indicate the formation of several low-symmetric niobate phases.

In this paper the valence of the Nb ions which influences the ionic radius and the charge compensation mechanism were not considered. This will be examined in future investigations.

4. Conclusion

At low Nb_2O_5 concentrations (up to 2.5 mol %) the Nb ions are nearly completely (≈ 80%) incorporated in the $SrTiO_3$ phase formed during the thermal treatment. They occupy octahedrally co-ordinated titanium sites. A further increase of the Nb_2O_5 concentration leads to a decrease in the $SrTiO_3$ formation.

The excess Nb ions remain on distorted octahedral sites in the glassy matrix and form low-symmetry niobate phases.

Acknowledgements

We are grateful to Prof. W. Blau (FDS Dresden) for helpful discussions and to the Deutsche Forschungsgemeinschaft for financial support under contract HU491/2-1.

References

1. U. BANACH, Th. HÜBERT, B. FELLMUTH and E. HEGENBARTH, *Ferroelectrics* **100** (1989) 111.
2. Th. HÜBERT, B. OERTEL, D. HEINZE, in Schwerpunktprogramm "Sensorsysteme" , PTB-Berichte F-12 edited by H. Kunzmann (Braunschweig, 1994) 1.
3. Th. HÜBERT, U. BANACH and E. V. MOROSOVA, in Proceedings of the 15th International Congress on Glass, Leningrad 1989, edited by O. V. Mazurin, Vol. 1b, (Nauka, Leningrad, 1989) 255.
4. B. PEPLINSKI, Th. HÜBERT, M. WILLFAHRT and U. BANACH, *Mater. Sci. Forum* **228** (1996) 531.
5. A. G. McKALE, B. W. VEAL, A. P. PAULIKAS, S.-K. CHAN and G. S. KNAPP, *J. Amer. Chem. Soc.* **110** (1988) 3763.

Received 4 September 1995
and accepted 21 October 1996